Pharmacokinetic Analysis of Ramatroban Using a Recirculatory Model with Enterohepatic Circulation by Measuring Portal and Systemic Blood Concentration Difference in Sprague-Dawley and Eisai Hyperbilirubinemic Rats

Toshiya Moriwaki,[1] Hiroyuki Yasui,[2] and Akira Yamamoto[1,3]

Received December 26, 2003; accepted February 10, 2004

Purpose. The aim of this study was to characterize the *in vivo* pharmacokinetics with the enterohepatic circulation (EHC) and identify the role of multidrug resistance–associated protein 2 (MRP2/Mrp2) in biliary excretion and absorption of ramatroban, a thromboxane A_2 antagonist using a recirculatory model.

Methods. Ramatroban was intravenously or orally administered to Sprague-Dawley rats (SDR) and Eisai hyperbilirubinemic rats (EHBR). Portal and systemic blood and bile samples were collected, and the drug concentrations were analyzed by high-performance liquid chromatography (HPLC) to estimate various global and local moments.

Results. The bioavailability (*BA*) of ramatroban was estimated at 21.0% in SDR and 61.9% in EHBR. The local absorption ratio for the dosage after oral administration (F_a^{dosage}) and the single-pass local absorption ratio for EHC ($F_{a'}$) in the rats were similar and nearly 100%. The hepatic recovery ratio (F_h) and the single-pass biliary excretion ratio through the liver for the sum of ramatroban and its glucuronides (F_b) in EHBR were 61.4% and 8.88%, respectively, which differed considerably from those in SDR (15.0% and 22.4%). The difference in hepatic elimination between these strains would be caused, at least in part, by the reduced biliary excretion in EHBR, although the biliary excretion was not completely impaired.

Conclusions. Ramatroban may be excreted by multiple transport systems, followed by efficient enterohepatic reabsorption in both strains. The results suggest that ramatroban may not be susceptible to drug-drug interaction involving MRP2/Mrp2 in biliary excretion and absorption.

KEY WORDS: Eisai hyperbilirubinemic rats; enterohepatic circulation; P–S difference; ramatroban; recirculatory model.

INTRODUCTION

Ramatroban, chemically designated as 3(*R*)-[[(4-fluorophenyl) sulfonyl]amino]-1,2,3,4-tetrahydro-9H-carbazole-9-propanoic acid (Fig. 1) is a potent and selective receptor antagonist of thromboxane A_2, which is classified as an organic anion (1). This drug has been shown to be effective for treating allergic rhinitis accompanied by nasal obstruction with few adverse effects in patients and is widely used on the market in Japan (2). It has been reported that ramatroban exhibits dose-proportional oral exposure, no accumulation or inhibition of metabolism, and the incomplete bioavailability as a result of presystemic metabolism in rats (3,4). The metabolism of ramatroban is mediated by both oxidation and glucuronidation and yields rather hydrophilic metabolites that are predominantly excreted via the biliary/fecal route. In addition, a study using a linked-rat model revealed that a certain amount of ramatroban could undergo enterohepatic circulation (EHC). Thus, complex metabolic processes including biliary transport appear to be involved in the pharmacokinetics of ramatroban, although an in-depth analysis of these processes remains to be conducted.

During the past decades, much attention has been directed toward the role of transporters in absorption and disposition of various xenobiotics and their metabolites (5). In the process of biliary excretion, primary active transporters significantly contribute to the drug transport from hepatocytes to bile across the canalicular membranes. In particular, multidrug resistance–associated protein 2 (in humans, MRP2, ABCC2, or cMOAT; in rodents, Mrp2) localized in the bile canalicular membrane plays a pivotal role in the transport of a diverse range of organic anions, for example, glutathione conjugates, glucuronides, and nonconjugated organic anions (6,7). Considerable advances in the study of the biliary transport by MRP2/Mrp2 have been made mainly owing to the establishment of mutant rats such as Eisai hyperbilirubinemic rats (EHBR) derived from Sprague-Dawley rats (SDR) (8). EHBR are genetically deficient in Mrp2 and have been used for investigations of the mechanism of organic anion transport in the liver. EHBR also elucidated the expression of MRP2/Mrp2 in the brush border membrane of enterocytes

[1] Department of Biopharmaceutics, Kyoto Pharmaceutical University, Kyoto 607-8414, Japan.

[2] Department of Analytical and Bioinorganic Chemistry, Kyoto Pharmaceutical University, Kyoto, Japan.

[3] To whom correspondence should be addressed. (e-mail: yamamoto@mb.kyoto-phu.ac.jp)

ABBREVIATIONS: EHC, enterohepatic circulation; R_b, partition ratio between whole blood and plasma; f_u, plasma free fraction; $\tilde{\delta}(s)$, impulse transfer function; $\tilde{C}_s^{iv}(s)$, Laplace transform of the systemic blood concentration after intravenous administration; $s\tilde{A}_a^{iv}(s)$, Laplace transform of the local absorption rate after intravenous administration; $s\tilde{A}_a^{po}(s)$, Laplace transform for the sum of local absorption rates for the dosage and EHC after oral administration; $\tilde{f}_h(s)$, transfer function for the liver; $\tilde{f}_c(s)$, transfer function for a single pass of EHC; $\tilde{f}_a^{dosage}(s)$, transfer function for local absorption for the dosage after oral administration; F_a^{iv}, recirculatory local absorption ratio for EHC after intravenous administration; F_a^{po}, the sum of the local absorption ratios for the dosage and recirculatory local absorption ratio for EHC after oral administration; F_a^{dosage}, local absorption ratio for the dosage after oral administration; F_a^{ehc}, recirculatory local absorption ratio for EHC after oral administration; F_h, hepatic recovery ratio; F_c, recovery ratio through a single pass of EHC from the biliary excretion to the absorption; $F_{a'}$, single-pass local absorption ratio for EHC; F_b, single-pass biliary excretion ratio through the liver for the sum of unchanged and conjugated forms; *BA*, bioavailability, *MAT,* mean absorption time from the gastrointestinal tract to the systemic circulation; $\bar{t}_a^{iv}$, mean local absorption time for EHC after intravenous administration; $\bar{t}_a^{po}$, the sum of the mean local absorption times for the dosage and EHC after oral administration; $\bar{t}_c$, mean transit time for a single pass of EHC from the biliary excretion to the absorption; Q_h, total hepatic blood flow rate; Q_p, portal blood flow rate; Q_{ha}, hepatic arterial blood flow rate; CL_h, hepatic clearance; $A_{bile,u}(\infty)$, cumulative amount of unchanged form excreted into the bile; $A_{bile,g}(\infty)$, cumulative amount of conjugated form excreted into the bile.

0724-8741/04/0600-1055/0 © 2004 Plenum Publishing Corporation

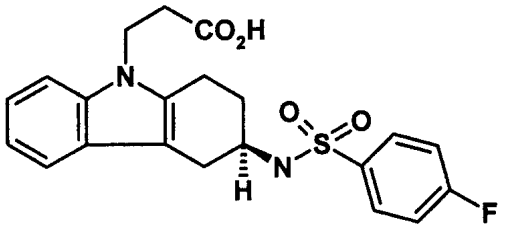

Fig. 1. Structure of ramatroban.

and identified its role in a detoxification system in the gastrointestinal tract (9).

To illustrate the complicated process of EHC, various pharmacokinetic models have been proposed (10). The recirculatory model, in which local drug dispositions in organs are treated as transfer functions characterized by input-output behavior in the Laplace domain is useful for EHC analysis, because the impact of EHC on global moments can be readily defined. Yamaoka *et al.* developed a simplified recirculatory model consisting of the two transfer functions (inside and outside the body) and applied the model to EHC analysis of some drugs (11–13). Recently, we have developed a general recirculatory model measuring portal and systemic blood concentration difference (P–S difference) after intravenous and oral administrations of drugs undergoing EHC (14). Because this model provides a relationship between global and local moments in each organ based on physiology, the local kinetics of EHC *in vivo* can be more strictly defined than that by the simplified model. In our previous study, the validity of the theory was experimentally confirmed by using cephradine as a model drug, which exhibited the complete absorption, renal excretion, bioavailability, and enterohepatic reabsorption. The extent and rate of EHC of cephradine were successfully analyzed by the theoretical equations in the Laplace domain using a program of nonlinear least-squares (MULTI) with fast inverse Laplace transform (FILT) (15). However, no attempt has yet been made to use this analysis for evaluation of a drug for which pharmacokinetics with EHC has not been fully investigated.

In the current study, in order to define the absorption, disposition, and EHC of ramatroban, we analyzed the P–S difference after intravenous and oral administrations in SDR using the recirculatory model. Ramatroban was also administered to EHBR to determine the role of MRP2/Mrp2 in the biliary excretion and intestinal secretion of the drug.

THEORY

Global and Local Moment Analysis of Ramatroban

According to the general recirculatory model for portal and systemic blood concentration differences described in the previous studies (14,16), the following equations for systemic or portal global zero-order moments can be derived, assuming that ramatroban is exclusively eliminated in the liver and undergoes EHC, and that the effect of drug disposition in the lung and gastrointestinal tract on the overall pharmacokinetics is negligible:

$$AUC_s^{iv} = \frac{D_{iv}}{CL_h} \tag{1}$$

$$AUC_p^{iv} = \frac{D_{iv}}{CL_h}\frac{Q_p + Q_{ha}F_c}{Q_p(1-F_c)} \tag{2}$$

$$CL_h = Q_h\left(1 - \frac{F_h}{1-F_c}\right) \tag{3}$$

$$AUC_s^{po} = \frac{D_{po}F_a^{dosage}F_h}{CL_h}\frac{1}{1-F_c} \tag{4}$$

$$AUC_p^{po} = \frac{D_{po}F_a^{dosage}}{Q_p}\frac{1}{1-F_c} + \frac{D_{po}F_a^{dosage}F_h}{CL_h}\frac{1}{1-F_c}\frac{Q_p + Q_{ha}F_c}{Q_p(1-F_c)} \tag{5}$$

where D_{iv} and D_{po} are the intravenous and oral doses, and Q_h, Q_p, and Q_{ha} are the hepatic, portal, and hepatic arterial blood flow rates ($Q_h = Q_p + Q_{ha}$). AUC_s^{iv} and AUC_p^{iv} are the areas under the systemic and portal concentration-time curves after intravenous administration, and AUC_s^{po} and AUC_p^{po} are the areas under the systemic and portal concentration-time curves after oral administration. CL_h is the hepatic clearance. F_c, F_h, and F_a^{dosage} are the recovery ratio through a single pass of EHC from biliary excretion to the absorption, the hepatic recovery ratio, and the local absorption ratio for the dosage after oral administration, respectively.

From Eqs. 1 through 5, various zero-order local moments can be expressed relative to global zero-order moments as follows:

$$F_h = \frac{D_{iv}AUC_s^{po}}{Q_p(AUC_p^{po}\,AUC_s^{iv} - AUC_s^{po}\,AUC_p^{iv})} \tag{6}$$

$$F_c = \frac{\alpha D_{iv} - Q_p AUC_s^{iv}(1-F_h)}{\alpha D_{iv} - Q_p AUC_s^{iv}} \tag{7}$$

$$F_a^{dosage} = \frac{D_{iv}Q_p AUC_s^{po}}{D_{po}(Q_p AUC_s^{iv} - \alpha D_{iv})} \tag{8}$$

where α is the ratio of Q_p to Q_h. In this study, an α value of 0.816 was used from the physiological data (14,16,17). F_c is a product of the single-pass biliary excretion ratio through the liver for the sum of unchanged and conjugated ramatroban (F_b) and the single-pass local absorption ratio for EHC ($F_{a'}$). The F_b value can be experimentally estimated by the following equation:

$$F_b = \frac{\alpha[A_{bile,u}(\infty) + A_{bile,g}(\infty)]}{Q_p AUC_s^{iv}(-)} \tag{9}$$

where $A_{bile,u}(\infty)$ and $A_{bile,g}(\infty)$ are the cumulative amounts of unchanged and conjugated ramatroban excreted into the bile, and $AUC_s^{iv}(-)$ is the systemic AUC after intravenous administration in bile duct-cannulated rats. The Q_p value required in Eqs. 6 to 9 is obtained by:

$$Q_p = \frac{D_{iv}[\alpha \cdot AUC_p^{po} + (1-\alpha)AUC_s^{po}]}{(AUC_p^{po}\,AUC_s^{iv} - AUC_s^{po}\,AUC_p^{iv})} \tag{10}$$

The equations for the bioavailability (BA), the recirculatory local absorption ratio for EHC after intravenous administration (F_a^{iv}), and the sum of the local absorption ratio for the dosage and recirculatory local absorption ratio for

EHC after oral administration ($F_a^{dosage} + F_a^{ehc} = F_a^{po}$) were previously described (14). Similarly, the equations between systemic or portal global first-order moment and the mean transit time for a single pass of EHC from biliary excretion to the absorption ($\bar{t}_c$), the mean local absorption time for EHC after intravenous administration ($\bar{t}_a^{iv}$), and the sum of the mean local absorption times for the dosage and EHC after oral administration ($\bar{t}_a^{po}$) were also given in the previous study (14).

Nonlinear Curve Fitting of the Local Absorption Rate and Simulation of Absorption Profiles for Dosage and EHC after Oral Administration of Ramatroban

From the general recirculatory model, the transfer function for the local absorption rate for EHC after intravenous administration

$$\left[\frac{dA_a^{iv}(t)}{dt}\right]$$

is defined as follows:

$$L\left[\frac{dA_a^{iv}(t)}{dt}\right] = s\tilde{A}_a^{iv}(s) = \tilde{C}_s^{iv}(s)Q_h\frac{\tilde{f}_c(s)}{1-\tilde{f}_c(s)} \tag{11}$$

where $s\tilde{A}_a^{iv}(s)$ is the Laplace transform of the local absorption rate, $\tilde{f}_c(s)$ is the transfer function for a single pass of EHC, and $\tilde{C}_s^{iv}(s)$ is the Laplace transform of the systemic blood concentration after intravenous administration provided by curve fitting of systemic blood concentrations according to a two-compartment model. A satisfactory result and the minimum Akaike's information criterion (AIC) value upon curve fitting with MULTI(FILT) were obtained in the following transfer function selected from among several models:

$$\tilde{f}_c(s) = e^{-t_0 s}F_c\left[\frac{a_1}{s+a_1}\frac{a_2}{s+a_2}\right] \tag{12}$$

where t_0 is the gap time, a_i is the exponent, and F_c derived from Eq. 7 was used for the fitting.

Similarly, the transfer function for the sum of local absorption rates for the dosage and EHC after oral administration

$$\left[\frac{dA_a^{po}(t)}{dt}\right]$$

can be defined as follows:

$$L\left[\frac{dA_a^{po}(t)}{dt}\right] = s\tilde{A}_a^{po}(s) = \left[D_{po} + \frac{D_{po}}{D_{iv}}\tilde{f}_h s\tilde{A}_a^{iv}(s)\right]\frac{\tilde{f}_a^{dosage}(s)}{1-\tilde{f}_c(s)} \tag{13}$$

where $s\tilde{A}_a^{po}(s)$ is the Laplace transform for the sum of local absorption rates for the dosage and EHC after oral administration, and $\tilde{f}_h(s)$ is the transfer function in the liver, which is assumed to be the product of F_h and impulse transfer function ($\tilde{\delta}(s)$). $\tilde{f}_a^{dosage}(s)$ is the transfer function for local absorption for the dosage after oral administration. Among several models, the following transfer function gave the most satisfactory result and the minimum AIC value upon curve fitting with MULTI(FILT):

$$\tilde{f}_a^{dosage}(s) = F_a^{dosage}\frac{a_3}{s+a_3}\left[\frac{Aa_4}{s+a_4} + \frac{(1-A)a_5}{s+a_5}\right] \tag{14}$$

where A is the coefficient.

The time profiles of the local absorption rates for the dosage

$$\left[\frac{dA_a^{dosage}(t)}{dt}\right]$$

and EHC

$$\left[\frac{dA_a^{ehc}(t)}{dt}\right],$$

the local absorption extent for the dosage

$$\left[\frac{A_a^{dosage}(t)}{D_{po}}\right],$$

the recirculatory local absorption extent for EHC

$$\left[\frac{A_a^{ehc}(t)}{D_{po}}\right],$$

and the sum of their absorption extents

$$\left[\frac{A_a^{po}(t)}{D_{po}}\right]$$

after oral administration are separately simulated using the previously defined Laplace transforms together with Eqs. 12 and 14 (14).

MATERIALS AND METHODS

Chemicals

Ramatroban and BAY w9990, an internal standard for high-performance liquid chromatography (HPLC) analysis, were a gift from Bayer Yakuhin, Ltd (Osaka, Japan). Acetonitrile, ether, and hexane were obtained from Nacalai Tesque, Inc. (Kyoto, Japan). Heparin was purchased from Novo Nordisk Ltd. (Bagsvaerd, Denmark). Glucose-6-phosphate, glucose-6-phosphate dehydrogenase, and $NADP^+$ were obtained from Wako Pure Chemical Industries (Osaka, Japan). All other chemicals and reagents used were of analytical grade.

Animal Experiments

The animal experiments were conducted in accordance with the "Principles of Laboratory Animal Care" (NIH Publication No. 85-23, revised 1985). SDR and EHBR weighing 200–220 g (Japan SLC, Inc, Shizuoka, Japan) were fasted with free access to water the night before the experiment. Ramatroban was dissolved in PEG400:water (1:1, v/v) for intravenous and oral administrations (2 mg/ml) and was administered intravenously or orally at a dose of 2 or 10 mg/kg to the rats. Under light anesthesia with ether, portal and systemic blood samples (1 ml) were simultaneously drawn from each rat with a heparinized syringe at 5, 10, 20, 30, and 45 min, and 1, 2, and 3 h after intravenous administration in SDR, at 5, 15, 30 min, and 1, 2, and 3 h after intravenous administration in EHBR, or at 10, 20, 30 min, and 1, 2, 4, 6, and 8 h after oral administration in SDR and EHBR. All blood samples were centrifuged at 3000 rpm for 10 min to obtain plasma samples.

An experiment using bile duct–cannulated rats was performed by the following procedure. The bile duct in male SDR and EHBR weighing 230–250 g was cannulated with a polyethylene tube (SP-10; Natsume, Tokyo, Japan) under anesthesia with ether. The femoral vein was also cannulated with an SP-50 polyethylene tube (Natsume). After the operation, each rat was kept in a Bollman cage with free access to water. After intravenous administration of ramatroban at 2 mg/kg, bile samples were periodically collected over a 5 h period into pre-weighed 1.5 ml tubes at 4°C. Plasma samples were also obtained at specified time points. These samples were stored at –20°C until analysis.

In vitro Studies

Partitioning of Ramatroban Between Whole Blood and Plasma

Partition ratio between whole blood and plasma (R_b) of ramatroban was measured using heparinized whole blood *in vitro* (16,17). After preincubation of the blood for 5 min at 37°C, a small volume of ramatroban solution was added to give a final concentration of 0.5 μg/ml. After incubation for 15 min at 37°C, the blood samples were centrifuged at 3000 rpm for 10 min to obtain plasma samples. The ramatroban concentrations in these plasma samples were measured by HPLC. The blood concentrations were obtained by multiplying the plasma concentrations by the R_b ratio. After this experiment, it was confirmed that no difference existed in hematocrit between SDR and EHBR.

Plasma Free Fraction of Ramatroban

Plasma free fraction (f_u) of ramatroban was determined in SDR and EHBR plasma by the equilibrium dialysis method in triplicate. A small volume of ramatroban solution was mixed with the rat plasma to give a concentration of 0.5 μg/ml. The mixture (1 ml) was subjected to equilibrium dialysis against 3 ml of pH 7.4 isotonic phosphate buffer using a dialysis membrane (Spectra/Por Biotech membranes) with a molecular mass cutoff of 15 kDa (Spectrum Industries, Los Angeles, CA, USA) for 6 h at 37°C. The plasma (0.1 ml) and buffer solution (2 ml) were removed and analyzed by HPLC. The recovery of ramatroban after the experiment was over 95%.

Preparation of Rat Liver Microsomes

Liver specimens from male SDR and EHBR were rinsed with ice-cold physiological saline and homogenized in 50 mM potassium phosphate buffer at pH 7.4 containing 0.1 mM EDTA using a glass-Teflon manual homogenizer in an ice-cold container. The homogenate was centrifuged at 9000 × *g* for 15 min at 4°C, and the supernatant was then centrifuged at 100,000 × *g* for 60 min at 4°C. The microsomal pellet obtained was resuspended in the phosphate buffer to 20 mg protein/ml and stored at –80°C.

Ramatroban Metabolism in Rat Liver Microsomes

Ramatroban (0.3 to 100 μM) was incubated with a reaction mixture (2 ml) consisting of 0.2 mg protein/ml microsomes prepared from SDR or EHBR and a NADPH-generating system (1.25 mM $NADP^+$, 5 mM glucose-6-phosphate, 2 U/ml glucose-6-phosphate dehydrogenase, and 10 mM $MgCl_2$) in 100 mM sodium phosphate buffer (pH 7.4). After preincubation for 3 min at 37°C, the reaction was initiated by addition of ramatroban dissolved in methanol (less than 1%, v/v). At the specified time points, 0.2 ml of the mixture was taken, and the reaction was terminated by addition of 50 μl of 1 N HCl. The experiments were performed in triplicate.

Analytical Procedures

For the determination of ramatroban, an aliquot of plasma (0.1 ml), bile diluted 100-fold with water (0.5 ml), or other samples from protein binding and metabolic experiments was added to 10 μl of internal standard (100 μg/ml of BAY w9990) dissolved in methanol, 50 μl of 1 N HCl, and 0.5 ml of water. For ramatroban liberation from the glucuronides, 20 μl of 1 N NaOH was added to the bile samples (0.1 ml) which were kept at room temperature for 1 h before the 100-fold dilution process. The mixture was vortexed for 3 min with 7 ml of ether:hexane (1:1, v/v) in a disposable glass test tube and centrifuged at 3000 rpm for 5 min. The organic layer was then transferred to another test tube and evaporated under a nitrogen stream at 40°C. The residue was reconstituted with 250 μl of mobile phase for HPLC and 150 μl of the solution was injected into a HPLC system. The HPLC system (LC-10AD; Shimadzu, Kyoto, Japan) was equipped with a UV detector (SPD-10A; Shimadzu) adjusted at 228 nm and an integrated data analyzer (Chromatopac CR7A; Shimadzu). The column was a Capcell Pak UG120 ODS reversed-phase column (5 μm, 4.6 mm i.d. × 250 mm; Shiseido, Tokyo, Japan) with a short preguard column (Capcell Pak, 4.6 mm i.d. × 20 mm; Shiseido). The mobile phase was composed of 5 mM pH 7.4 potassium dihydrogenphosphate (72%, v/v) and acetonitrile (28%, v/v). The flow rate was 1 ml/min, and the column temperature was 40°C. The limits of quantification of ramatroban in plasma, bile, and the other specimens were 0.02, 0.5, and 0.002 to 0.02 μg/ml, respectively. All correlation coefficients of the calibration curves were around 0.999, and the precision and accuracy of inter-day assay were within 10%.

Data Analysis

Calculation of in vivo Pharmacokinetic Parameters

The blood concentration and biliary excretion data were expressed as arithmetic mean and standard deviation (SD) with n = 3 to 4 in SDR and n = 3 in EHBR. *AUC* and *MRT* were calculated by log trapezoidal integration with extrapolation to infinite time. The CL_n and volume of distribution at steady-state (V_{ss}) were calculated from *AUC* and *MRT* values. The MULTI(FILT) and FILTS programs in Microsoft FORTRAN (ver. 3.2) were used for nonlinear curve fitting of absorption rate profiles after intravenous and oral administrations and for simulation of the local absorption rates and extents for the dosage and EHC after oral administration, respectively (15).

Calculation of in vitro CL_{int}

The Michaelis-Menten parameters of K_m and V_{max} were determined as an index of oxidation metabolism using the

metabolic disappearance of ramatroban in microsomes prepared from SDR and EHBR. The equation for Michaelis-Menten kinetics was used for the fitting of the initial metabolic rates to obtain the kinetic parameters using MULTI (18). The CL_{int} values were determined by dividing V_{max} by K_m. The Student's t test was used to evaluate significant differences in parameters between SDR and EHBR, and a p value of less than 0.05 was considered to be statistically significant.

RESULTS

The portal and systemic blood concentration-time profiles of ramatroban after intravenous and oral administrations at 2 and 10 mg/kg in SDR and EHBR are shown in Fig. 2, and the corresponding global moments are listed in Table I. Following intravenous dosing to SDR, systemic blood concentrations of ramatroban declined poly-exponentially, whereas bi-exponential elimination was observed in EHBR. No blood concentrations for the glucuronides were detected in either group of rats. The blood concentration of ramatroban in SDR at each time point was lower than that in EHBR, resulting in a 3-fold greater CL_h (2.68 vs. 0.896 $L \cdot h^{-1} \cdot kg^{-1}$). The V_{ss} values in SDR and EHBR were 0.496 and 0.848 L/kg. The terminal $t_{1/2}$ in SDR was calculated to be 0.427 h, which was approximately 2-fold shorter than that in EHBR (0.743 h). The portal blood concentrations in SDR and EHBR were higher than the systemic blood concentrations particularly in the later phase, and the P–S difference was especially pronounced in SDR. As a result, the portal AUC was greater than the systemic AUC in both strains (1.05 vs. 0.747 μg·h/ml in SDR, 2.49 vs. 2.23 μg·h/ml in EHBR). The SDR exhibited longer portal MRT than systemic MRT (0.877 vs. 0.370 h), whereas the portal MRT was comparable to the systemic MRT in EHBR (0.947 vs. 1.03 h). Following oral dosing, a remarkable P–S difference was observed in both strains (Fig. 2). Therefore, the portal AUC values were about 8-fold higher in SDR and 2-fold higher in EHBR than the corresponding systemic AUC values, respectively (Table I).

Table II lists various local moments obtained from Eqs. 6 to 9 and the reported equations. Consistent with the difference in CL_h, the calculated BA in SDR (21.0%) was considerably lower than that in EHBR (61.9%). Because nearly complete absorption was achieved in both strains as indicated by the F_a^{dosage} values, the difference in BA was attributed to a lower F_h in SDR than that in EHBR. Both F_a^{iv} and F_a^{po} in SDR were greater than those in EHBR because of the higher F_c value in SDR. The study in bile duct–cannulated rats revealed that ramatroban exhibited an F_b of 22.4% in SDR and 8.88% in EHBR, which accounted for the rather different F_c values, given a comparable $F_{a'}$ of >90% in the two strains. For the first order moments, the $\bar{t}_a^{iv}$, MAT, and $\bar{t}_a^{po}$ values in SDR were

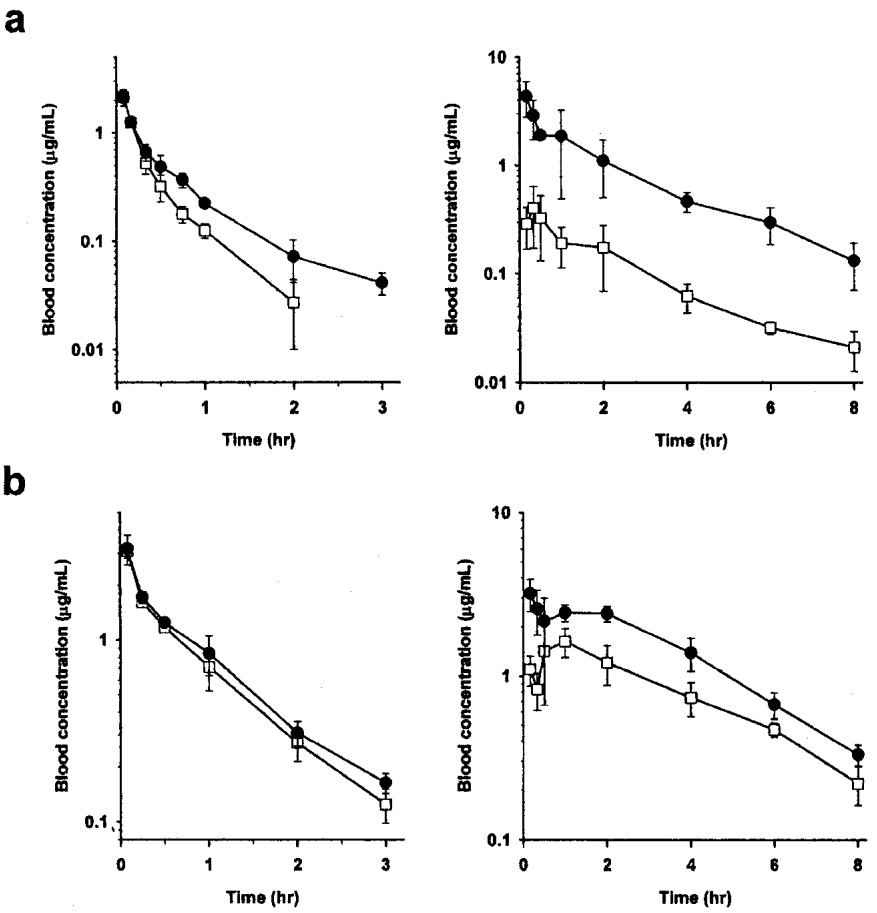

Fig. 2. The portal (●) and systemic (□) blood concentration-time profiles after intravenous (left panel) and oral (right panel) administration of ramatroban at doses of 2 and 10 mg/kg in (a) SDR and (b) EHBR, respectively. Each point represents mean ± SD value (n = 3 to 4).

Table I. Global Moments of Portal and Systemic Blood Concentration Profiles after Intravenous (2 mg/kg) and Oral (10 mg/kg) Administration of Ramatroban in SDR and EHBR

		SDR		EHBR	
		Portal	Systemic	Portal	Systemic
A. Intravenous administration					
AUC	(μg·h/ml)	1.05	0.747	2.49	2.23
MRT	(h)	0.877	0.370	1.03	0.947
CL_h	($L \cdot h^{-1} \cdot kg^{-1}$)	—	2.68	—	0.896
V_{ss}	(L/kg)	—	0.496	—	0.848
B. Oral administration					
AUC	(μg·h/ml)	6.23	0.783	12.2	6.91
MRT	(h)	2.74	2.95	3.48	3.82

Results are estimated from the mean concentration profiles, each point of which is expressed as the mean value of 3–4 rats. SDR, Sprague-Dawley rats; EHBR, Eisai hyperbilirubinemic rats.

in similar ranges of those in EHBR, while a 2-fold increase in $\bar{t}_c$ was noted in SDR from that in EHBR (1.34 vs. 0.763 h).

On the basis of Eq. 11, the time profiles of local absorption rate of EHC after intravenous administration in SDR and EHBR were fitted with MULTI(FILT) as shown in Fig. 3. A satisfactory result for curve fitting was obtained by using Eq. 12 with values of t_0, a_1, and a_2 of 0.150 h, 244 h^{-1}, and 1.40 h^{-1} for SDR and 0 h, 1.24×10^5 h^{-1}, and 1.51 h^{-1} for EHBR, respectively. Similarly, the observed values of the sum of the local absorption rate profiles for the dosage and EHC after oral administration were well fitted using Eq. 13 and Eq. 14, where a_3, a_4, a_5, and A were 7.21 h^{-1}, 15.7 h^{-1}, 0.399 h^{-1}, and 0.263 for SDR, and 1.33×10^4 h^{-1}, 6.48 h^{-1}, 0.277 h^{-1}, and 0.116 for EHBR, respectively (Fig. 3). The time profiles of local absorption rates for the dosage and EHC are also shown in Fig. 3. The local absorption rates for the dosage showed a bi-phasic decrease, whereas the local absorption rates for EHC reached a maximum at 1 to 2 h, followed by a similar decrease to the local absorption rates for the dosage in both SDR and EHBR. Using the same fitting equations, the time profiles of local absorption extent for the dosage, recirculatory local absorption extent for EHC, and the sum of their absorption extents after oral administration are simulated in Fig. 4. The simulated curves for the sum of the local absorption extents were almost superimposed on the observed values in both strains.

Table II. Local Moments Calculated from Blood Concentrations and Biliary Excretions of Ramatroban in SDR and EHBR

		SDR	EHBR
F_a^{iv}	(%)	40.8	29.0
F_a^{po}	(%)	143	127
F_a^{dosage}	(%)	105	92.0
F_a^{ehc}	(%)	43.0	26.7
F_h	(%)	15.0	61.4
F_c	(%)	24.6	8.70
F_b*	(%)	22.4	8.88
$F_{a'}$	(%)	110	99.2
BA	(%)	21.0	61.9
MAT	(h)	2.58	2.87
$\bar{t}_a^{iv}$	(h)	2.14	1.78
$\bar{t}_a^{po}$	(h)	2.71	3.05
$\bar{t}_a^{dosage}$	(h)	2.15	2.83
$\bar{t}_c$	(h)	1.34	0.763

Results are estimated from the mean concentration profiles, each point of which is expressed as the mean value of 3–4 rats. SDR, Sprague-Dawley rats; EHBR, Eisai hyperbilirubinemic rats.
* Estimated from data in bile duct-cannulated rats.

Table III lists the cumulative biliary excretion of ramatroban and its glucuronides after intravenous administration at 2 mg/kg in bile duct–cannulated SDR and EHBR. Both strains showed biliary excretion of ramatroban and its glucuronides. A similar range of $A_{bile,u}(\infty)$ was observed in SDR and EHBR (320 ± 69.1 vs. 262 ± 42.1 μg/kg), whereas $A_{bile,g}(\infty)$ in SDR was significantly greater than that in EHBR ($p < 0.05$). Consequently, total biliary excretion in SDR and EHBR was calculated to be 28.5 ± 2.6 and 20.0 ± 1.3% of dose, respectively. Table IV lists *in vitro* estimates, the R_b ratio and f_u. The R_b ratio in EHBR was significantly higher than that in SDR ($p < 0.05$). The f_u of ramatroban was relatively low with 1.2% and was almost similar between the two strains. Figure 5 depicts the relationship between metabolic rate calculated from initial disappearance of ramatroban and substrate concentration in liver microsomes. Saturated profiles were observed for metabolic rates in both rats, which were well fitted by the Michaelis-Menten equation. Although the K_m values were comparable, V_{max} in EHBR was 5-fold lower than that in SDR (0.265 ± 0.0288 vs. 1.41 ± 0.200 $nmol \cdot min^{-1} \cdot mg^{-1}$ protein), resulting in a significant difference in CL_{int} ($p < 0.05$) as shown in Table V.

DISCUSSION

In the current study, a general recirculatory model with EHC for the P–S difference was used to analyze the pharmacokinetics of ramatroban. The study also intended to investigate the effect of MRP2/Mrp2 on the *in vivo* pharmacokinetics of ramatroban after intravenous and oral administrations to both SDR as control rats and EHBR as Mrp2 deficient rats. The results indicated that ramatroban is excreted in its unchanged and conjugated forms via the bile duct, and these forms are almost completely absorbed from the gastrointestinal tract into the portal system in both strains. The hepatic recovery ratio in EHBR was found to be much higher than that in SDR due to large decreases in the oxidation metabolism and biliary excretion of ramatroban in EHBR. Recently, Chen *et al.* conducted a study using the P–S difference after oral administration in SDR and EHBR to investigate the role of MRP2/Mrp2 in the absorption of several organic anions (19). However, that study did not take into account the effect of EHC on the P–S difference after oral dosing. The advantage of our study over their study was independent definition of absorption from the dosage and EHC.

After intravenous administration of ramatroban to SDR, systemic and portal blood concentrations were comparable in the initial phase, but the P–S difference increased as time elapsed (Fig. 2). This increase was accounted for by the gap time variable of Eq. 12. These findings suggest that a time delay exists in the biliary excretion and/or reabsorption process of EHC. Conversely, EHBR exhibited no gap time for EHC. The reason for this difference is obscure and remains to be clarified by further investigation. As a consequence, F_a^{iv} was estimated at 40.8% in SDR and 29.0% in EHBR (Table II). An almost identical contribution of EHC to local absorp-

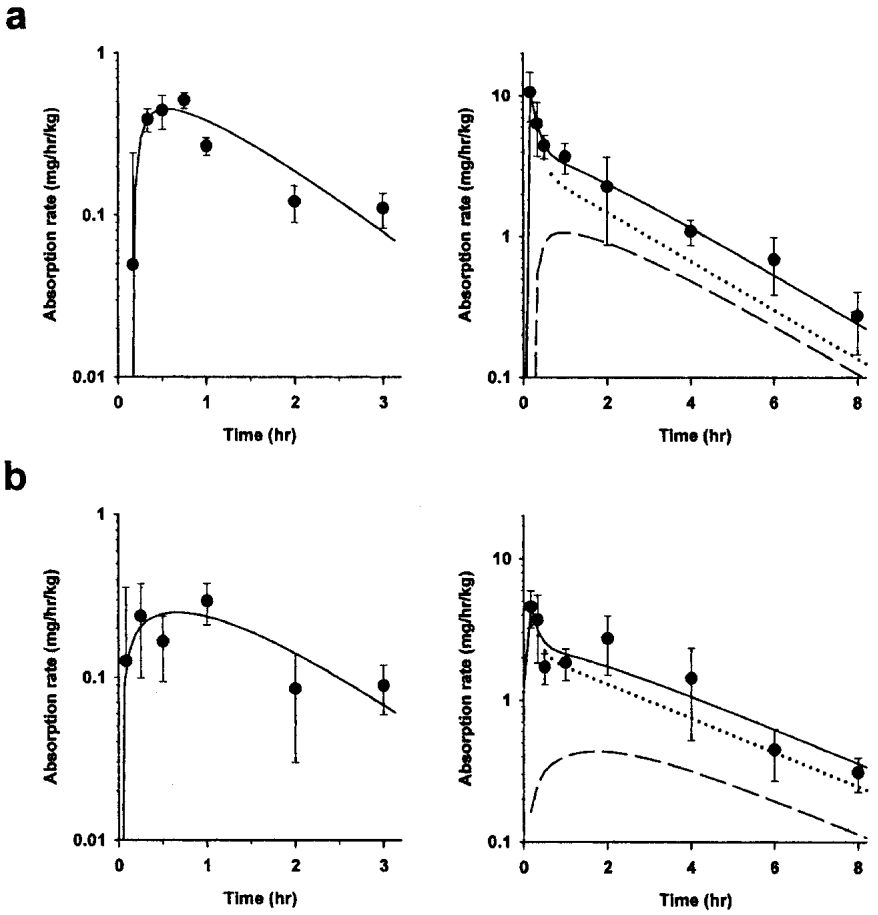

Fig. 3. The local absorption rate time-profiles of ramatroban from the gastrointestinal tract into the portal system after intravenous (left panel) and oral (right panel) administration at doses of 2 and 10 mg/kg in (a) SDR and (b) EHBR, respectively. The symbol (●) and solid lines represent observed and theoretical values of the local absorption rate (left panel) and sum of the local absorption rates for the dosage and EHC (right panel), respectively. The dotted and semi-dotted lines represent the simulated local absorption rates for the dosage and EHC, respectively. Each point represents mean ± SD value (n = 3 to 4). The lines of the total local absorption rates were obtained by curve fittings based on Eqs. 11 and 13 substituted with Eqs. 12 and 14, where t_0, a_1, a_2, a_3, a_4, a_5, and A are 0.150 h, 244 h^{-1}, 1.40 h^{-1}, 7.21 h^{-1}, 15.7 h^{-1}, 0.399 h^{-1}, and 0.263 for SDR, and 0 h, 1.24×10^5 h^{-1}, 1.51 h^{-1}, $1.33 \cdot 10^4$ h^{-1}, 6.48 h^{-1}, 0.277 h^{-1}, and 0.116 for EHBR, respectively. The lines of the local absorption rate for the dosage and EHC were simulated on the basis of the published equations (14).

tion was observed after oral administration as indicated by F_a^{ehc} of 43.0 and 26.7% in SDR and EHBR, respectively. In our previous study using cephradine as a model drug, F_a^{ehc} (71.5%) was much higher than F_a^{iv} (45.0%) (14). This discrepancy can be explained by a difference in elimination routes for the two drugs. For cephradine, the renal clearance accounts for the total body clearance and *BA* is complete because $F_{a'}$ and F_a^{dosage} are 100% and F_h is equal to $1–F_b$. In contrast, the hepatic metabolism is the predominant elimination route for ramatroban. Therefore, in the case of cephradine, F_a^{iv} and F_a^{ehc} can be expressed using local moments deduced from the general recirculatory model as follows:

$$F_a^{iv} = \frac{F_b Q_h}{CL_r(1 - F_b)} \tag{15}$$

$$F_a^{ehc} = \frac{F_b(Q_h + CL_r)}{CL_r(1 - F_b)} \tag{16}$$

Similarly, for ramatroban,

$$F_a^{iv} = \frac{F_{a'} F_b}{1 - F_{a'} F_b - F_h} \tag{17}$$

$$F_a^{ehc} = \frac{F_a^{dosage} F_{a'} F_b}{1 - F_{a'} F_b - F_h} \tag{18}$$

Thus, it is noteworthy that F_a^{ehc} is always higher than F_a^{iv} for drugs such as cephradine, whereas F_a^{ehc} cannot exceed F_a^{iv} for drugs showing exclusive hepatic elimination such as ramatroban.

For ramatroban, we found that not only F_a^{dosage} but also $F_{a'}$ was nearly 100% in intact SDR and EHBR (Table II). Boberg *et al.* (3) reported that the extent of absorption of radiolabeled ramatroban amounted to 83% post oral dosing in bile duct–cannulated rats, suggesting that ramatroban can be completely absorbed. This observation is in agreement

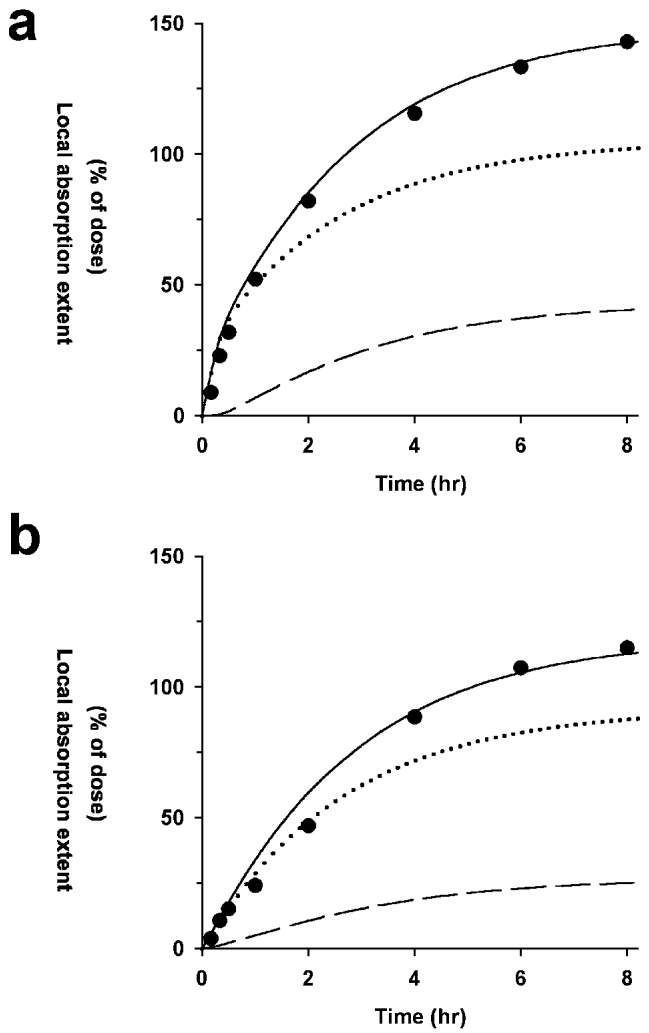

Fig. 4. The local absorption extent-time profiles of ramatroban from the gastrointestinal tract into the portal system (% of dose) after oral administration at a dose of 10 mg/kg in (a) SDR and (b) EHBR. The symbol (●) and solid line represent observed and simulated values of the sum of the local absorption extents, respectively. The dotted and semi-dotted lines represent the simulated local absorption extent for the dosage and recirculatory local absorption extent for EHC. Each point represents the mean value (n = 3 to 4). The lines were simulated on the basis of the published equations (14).

with our data. Using a linked-rat model, they showed that only 16.5% of the initial dose of radiolabeled ramatroban was reabsorbed from the gastrointestinal tract during the first circulation through EHC. However, it should be noted that ramatroban undergoes oxidation as well as glucuronidation in the liver, thereby forming many oxidative metabolites that cannot permeate through the gastrointestinal tract. Therefore, the difference in these two findings is not contradictory. Maximal $F_{a'}$ implies that all the glucuronides excreted from the bile can be converted to ramatroban in the gastrointestinal tract, contributing to EHC. A similar conclusion was made by Lin *et al.,* who observed EHC of diflunisal subsequent to biliary excretion as its acyl glucuronides (20). MRP2/Mrp2 has been shown to play an important role in the secretion of some organic anions from the gastrointestinal tract by *in vitro* techniques, possibly leading to incomplete F_a^{dosage} and/or $F_{a'}$ *in vivo* situation (9). However, our findings of complete F_a^{dosage} and $F_{a'}$ suggest that the effect of intestinal secretion by MRP2/Mrp2 on the pharmacokinetics of ramatroban may be minimal. This is supported by a recent report in which the absorption of MRP2/Mrp2 substrates, probenecid, and methotrexate was similar between SDR and EHBR *in vivo*, despite the significant impairment of biliary excretion in EHBR (19). The low expression of MRP2/Mrp2 in the intestine compared to that in the liver may explain these phenomena (21).

The total biliary excretion in EHBR was significantly lower than that in SDR, and F_b in EHBR decreased by 2.5-fold compared with that in SDR. However, biliary excretion was not entirely abolished in EHBR (Table III). Collectively, these data demonstrate that ramatroban along with its glucuronides may be transported by, at least in part, MRP2/Mrp2,

Table III. Cumulative Biliary Excretion of Ramatroban and its Glucuronides after Intravenous Administration at a Dose of 2 mg/kg in Bile Duct–Cannulated SDR and EHBR (mean ± SD, n = 3)

		SDR	EHBR
$A_{bile,u}(\infty)$	(μg/kg)	320 ± 69.1	262 ± 42.1
$A_{bile,g}(\infty)$	(μg/kg)	250 ± 36.6[a]	138 ± 16.0
Total biliary excretion	(% of dose)	28.5 ± 2.6[a]	20.0 ± 1.3

SDR, Sprague-Dawley rats; EHBR, Eisai hyperbilirubinemic rats.
[a] $p < 0.05$ compared with the value in EHBR.

Table IV. Partition Ratio Between Whole Blood and Plasma (R_b) and Plasma-Free Fraction (f_u) of Ramatroban in SDR and EHBR (mean ± SD)

		SDR	EHBR
R_b[a]		0.630 ± 0.015[c]	0.664 ± 0.021
f_u[b]	(%)	1.16 ± 0.19	1.20 ± 0.16

SDR, Sprague-Dawley rats; EHBR, Eisai hyperbilirubinemic rats.
[a] n = 6–10.
[b] n = 3.
[c] $p < 0.05$ compared with the value in EHBR.

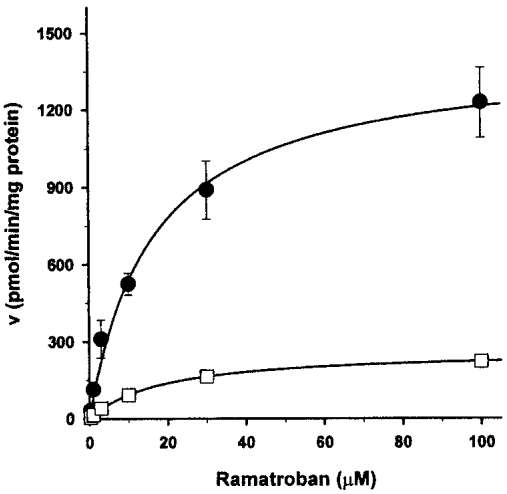

Fig. 5. The relationship between metabolic rate (v) and ramatroban concentration in liver microsomes prepared from SDR (●) and EHBR (□). The symbol and solid lines represent observed and theoretical values. Each point represents mean ± SD value (n = 3).

Table V. Enzyme Kinetic Parameters of Ramatroban in SDR and EHBR (mean ± SD, n = 3)

		SDR	EHBR
K_m	(μM)	16.3 ± 7.5	18.4 ± 4.4
V_{max}	(nmol·min^{-1}·mg protein)	1.41 ± 0.200[a]	0.265 ± 0.0288
CL_{int}	(ml·min^{-1}·mg protein)	0.0952 ± 0.0277[a]	0.0159 ± 0.0192

SDR, Sprague-Dawley rats; EHBR, Eisai hyperbilirubinemic rats.
[a] $p < 0.05$ compared with the value in EHBR.

and the transporters other than MRP2/Mrp2 may also be involved in the biliary transport. Similar data were reported previously for some organic anions (22–24). These reports concluded that a multiplicity of biliary excretion mechanism could account for the results. Indepth kinetic studies using bile canalicular membrane vesicles will be required for the characterization of the biliary excretion mechanisms of ramatroban and its glucuronides.

Given that comparable enterohepatic reabsorption was observed in SDR and EHBR, it was speculated that the large difference in CL_h between these strains could be due to other mechanisms than low biliary clearance in EHBR. A recent study showed that Mrp3 is induced in on the sinusoidal membrane of hepatocytes in EHBR, whereas it is not expressed in normal rat liver (5). If ramatroban is a substrate of Mrp3, active efflux by the transporter could cause low clearance in EHBR. A difference in clearance due to oxidative metabolism in the two strains may also explain the variation in CL_h. As shown in Fig. 5, the metabolic rate in liver microsomes prepared from SDR was appreciably higher than that from EHBR at any substrate concentration. From these data, metabolic parameters (V_{max}, K_m, *and* CL_{int}) were defined using MULTI. Whereas the K_m values in SDR and EHBR were in the same range, the V_{max} in EHBR was reduced by 5-fold from that in SDR (Table V), resulting in a significant difference in CL_{int} between the two strains. These results indicate that one of the reasons for the lower CL_h in EHBR is a considerable decrease in the oxidation capacity of ramatroban. Ohmori *et al.* (25) reported that the testosterone 6β-hydoxylase activity mediated by rat CYP3A is significantly decreased in EHBR, which would support our findings because ramatroban is also a CYP 3A substrate (unpublished data). The V_{ss} of ramatroban in EHBR was 2-fold higher than that in SDR. A similar disparity in V_{ss} was recently found for pitavastatin (26). Furthermore, the R_b ratio in EHBR was slightly but significantly higher than that in SDR. Thus, there appear to be various differences in physiology influencing pharmacokinetics between SDR and EHBR, other than hepato-biliary functions (27).

In conclusion, the pharmacokinetic analysis using the recirculatory model demonstrated that ramatroban may be excreted by multiple transport mechanisms from the bile, and excretion is followed by efficient enterohepatic reabsorption. These results suggest that ramatroban is not likely to be involved in drug-drug interaction involving MRP2/Mrp2 during biliary excretion and absorption.

REFERENCES

1. J. G. Theis, H. Dellweg, E. Perzborn, and R. Gross. Binding characteristics of the new thromboxane A_2/prostaglandin H_2 receptor antagonist [3H]BAY u3405 to washed human platelets and platelet membranes. *Biochem. Pharmacol.* **44**:495–503 (1992).
2. Y. Motobayashi, W. Imagawa, and K. Saida. Ramatroban (Baynas): a review of its pharmacological and clinical profile. *Folia Pharmacol. Jpn.* **118**:397–402 (2001).
3. M. Boberg, H. J. Ahr, B. Beckermann, K. Bühner, H. M. Siefert, W. Steinke, C. Wünsche, and M. Hirayama. Pharmacokinetics and metabolism of the new thromboxane A_2 receptor antagonist ramatroban in animals. *Arzneimittelforschung* **47**:928–938 (1997).
4. W. Steinke, H. J. Ahr, and M. Hirayama. Pharmacokinetics and metabolism of the new thromboxane A_2 receptor antagonist ramatroban in animals. 2nd communication: distribution to organs and tissues in male, female and pregnant rats, and characteristics of protein binding in plasma. *Arzneimittelforschung* **47**:939–948 (1997).
5. H. Kusuhara and Y. Sugiyama. Role of transporters in the tissue-selective distribution and elimination of drugs: transporters in the liver, small intestine, brain and kidney. *J. Control. Rel.* **78**:43–54 (2002).
6. J. König, A. T. Nies, Y. Cui, I. Leier, and D. Keppler. Conjugate export pumps of the multidrug resistance protein (MRP) family: localization, substrate specificity, and MRP2-mediated drug resistance. *Biochim. Biophys. Acta* **1461**:377–394 (1999).
7. D. Keppler, T. Kamisako, I. Leier, Y. Cui, A. T. Nies, and H. Tsujii. and J. König. Localization, substrate specificity, and drug resistance conferred by conjugate export pumps of the MRP family. *Adv. Enzyme Regul.* **40**:339–349 (2000).
8. S. Hosokawa, O. Tagaya, T. Mikami, Y. Nozaki, A. Kawaguchi, K. Yamatsu, and M. Shamoto. A new rat mutant with chronic conjugated hyperbilirubinemia and renal glomerular lesions. *Lab. Anim. Sci.* **42**:27–34 (1992).
9. Y. Gotoh, H. Suzuki, S. Kinoshita, T. Hirohashi, Y. Kato, and Y. Sugiyama. Involvement of an organic anion transporter (canalicular multispecific organic anion transporter/multidrug resistance-associated protein 2) in gastrointestinal secretion of glutathione conjugates in rats. *J. Pharmacol. Exp. Ther.* **292**:433–439 (2000).
10. M. S. Roberts, B. M. Magnusson, F. J. Burczynski, and M. Weiss. Enterohepatic circulation: physiological, pharmacokinetic and clinical implications. *Clin. Pharmacokinet.* **41**:751–790 (2002).
11. K. Yamaoka, M. Kanba, Y. Toyoda, Y. Yano, and T. Nakagawa. Analysis of enterohepatic circulation of cefixime in rat by fast inverse Laplace transform (FILT). *J. Pharmacokinet. Biopharm.* **18**:545–559 (1990).
12. T. Fukuyama, K. Yamaoka, Y. Ohata, and T. Nakagawa. A new analysis method for disposition kinetics of enterohepatic circulation of diclofenac in rats. *Drug Metab. Dispos.* **22**:479–485 (1994).
13. H. Yasui, K. Yamaoka, and T. Nakagawa. Moment analysis of stereoselective enterohepatic circulation and unidirectional chiral inversion of ketoprofen enantiomers in rat. *J. Pharm. Sci.* **85**:580–585 (1996).
14. T. Moriwaki, H. Yasui, and A. Yamamoto. A recirculatory model with enterohepatic circulation by measuring portal and systemic blood concentration difference. *J. Pharmacokinet. Pharmacodyn.* **30**:119–144 (2003).
15. Y. Yano, K. Yamaoka, and H. Tanaka. A nonlinear least squares program, MULTI(FILT), based on fast inverse Laplace transform for microcomputers. *Chem. Pharm. Bull.* **37**:1035–1038 (1989).
16. T. Moriwaki, H. Yasui, Y. Shigemoto, and N. H. Yoshida. A recirculatory model for local absorption and disposition of ciprofloxacin by measuring portal and systemic blood concentration difference. *J. Pharm. Sci.* **91**:196–205 (2002).

17. J. H. Lin, Y. Sugiyama, S. Awazu, and M. Hanano. Physiological pharmacokinetics of ethoxybenzamide based on biochemical data obtained in vitro as well as on physiological data. *J. Pharmacokinet. Biopharm.* **10**:649–661 (1982).
18. K. Yamaoka, Y. Tanigawara, T. Nakagawa, and T. Uno. A pharmacokinetic analysis program (multi) for microcomputer. *J. Pharmacobiodyn.* **4**:879–885 (1981).
19. C. Chen, D. Scott, E. Hanson, J. Franco, E. Berryman, M. Volberg, and X. Liu. Impact of Mrp2 on the biliary excretion and intestinal absorption of furosemide, probenecid, and methotrexate using Eisai hyperbilirubinemic rats. *Pharm. Res.* **20**:31–37 (2003).
20. J. H. Lin, K. C. Yeh, and D. E. Duggan. Effect of enterohepatic circulation on the pharmacokinetics of diflunisal in rats. *Drug Metab. Dispos.* **13**:321–326 (1985).
21. A. D. Mottino, T. Hoffman, L. Jennes, and M. Vore. Expression and localization of multidrug resistant protein mrp2 in rat small intestine. *J. Pharmacol. Exp. Ther.* **293**:717–723 (2000).
22. Y. Sugiyama, Y. Kato, and X. Chu. Multiplicity of biliary excretion mechanisms for the camptothecin derivative irinotecan (CPT-11), its metabolite SN-38, and its glucuronide: role of canalicular multispecific organic anion transporter and P-glycoprotein. *Cancer Chemother. Pharmacol.* **42**(Suppl):S44–S49 (1998).
23. K. Niinuma, O. Takenaka, T. Horie, K. Kobayashi, Y. Kato, H. Suzuki, and Y. Sugiyama. Kinetic analysis of the primary active transport of conjugated metabolites across the bile canalicular membrane: comparative study of S-(2,4-dinitrophenyl)-glutathione and 6-hydroxy-5,7-dimethyl-2-methylamino-4-(3-pyridylmethyl)benzothiazole glucuronide. *J. Pharmacol. Exp. Ther.* **282**: 866–872 (1997).
24. A. Nishino, Y. Kato, T. Igarashi, and Y. Sugiyama. Both cMOAT/MRP2 and another unknown transporter(s) are responsible for the biliary excretion of glucuronide conjugate of the nonpeptide angiotensin II antagonist, telmisaltan. *Drug Metab. Dispos.* **28**:1146–1148 (2000).
25. S. Ohmori, S. Kuriya, T. Uesugi, T. Horie, F. Sagami, T. Mikami, A. Kawaguchi, T. Rikihisa, and Y. Kanakubo. Decrease in the specific forms of cytochrome P-450 in liver microsomes of a mutant strain of rat with hyperbilirubinuria. *Res. Commun. Chem. Pathol. Pharmacol.* **72**:243–253 (1991).
26. H. Fujino, I. Yamada, S. Shimada, and M. Yoneda. and J. Kojima. Metabolic fate of pitavastatin, a new inhibitor of HMG-CoA reductase-effect of cMOAT deficiency on hepatobiliary excretion in rats and of mdr 1a/b gene disruption on tissue distribution in mice. *Drug Metab. Pharmacokin.* **17**:449–456 (2002).
27. T. Inagaki, M. Hoshino, H. Ohara, T. Yamada, T. Ogasawara, H. Shimizu, and M. Itoh. Decreased pancreatic exocrine function in the mutant Eisai hyperbilirubinemic rat (EHBR). *Pancreas* **18**: 172–179 (1999).